MRS Communications (2024) 14:372–378

https://doi.org/10.1557/s43579-024-00550-7

MRS Communications

Research Letter

A calcium aluminum rhenium sodalite with reducible rhenium in the sodalite cage

Danrui Ni, Department of Chemistry, Princeton University, Princeton, NJ 08544, USA
Guangming Cheng, Princeton Materials Institute, Princeton University, Princeton, NJ 08544, USA
Lun Jin, and Chen Yang, Department of Chemistry, Princeton University, Princeton, NJ 08544, USA
Nan Yao, Princeton Materials Institute, Princeton University, Princeton, NJ 08544, USA
Robert J. Cava, Department of Chemistry, Princeton University, Princeton, NJ 08544, USA

Address all correspondence to Robert J. Cava at **rcava@princeton.edu**

(Received 11 January 2024; accepted 22 March 2024; published online: 12 April 2024)

Abstract

An unreported rhenium-based calcium aluminum sodalite (CARe sodalite) has been synthesized by a traditional solid-state method. The rhenium is located in the sodalite β-cage and can be reduced under 5% H_2 forming gas without breaking the cage framework. Preliminary characterizations of the structural, optical, and magnetic properties are reported.

Introduction

Zeolites are a class of inorganic microporous crystalline materials that have been studied extensively largely due to its wide-ranging applications. These studies have been done from chemical, geometrical, topological, and crystallographic perspectives.[1–4] Among zeolite-based materials, sodalites are the most widely studied.[3] These materials have a relatively simple charge-balanced crystal structure with an isotropic "β-cage"[5] and can be described by the general formula $M_8(ABO_4)_6{:}2X$, where M is Ca or Na, A and B are Al and Si, and X is a negatively charged individual ion or a negatively charged group of ions. Many sodalites are based on $Na_8Al_6Si_6O_{24}$ (sodium aluminosilicate) frameworks but some are known to be based on $M^{II}{}_8Al_{12}O_{24}$ (e.g., calcium aluminate) frameworks. The A and B species together, such as Al plus Si, form tetrahedra that link to form sodalite framework β-cages in the Na sodalites; the same being true when A and B are both Al in calcium aluminate sodalites. To stabilize the $Ca_8Al_{12}O_{24}$ framework of the Ca-Al-O sodalites, the cages must contain a strongly bonded group in the cage to generate charge neutrality—creating a material that is known for a number of anions (many of which are in an oxygen coordinated polyhedra, as $\boldsymbol{X}O_y^{2-}$), in particular from the Cr, Mo, W column of the periodic table, but also for S and Se.[6–9]

With their relatively simple but versatile framework and various chemical compositions, as well as their semi-condensed porous architectures, sodalites have been particularly widely studied. They have been used in catalysis, ion-exchange, adsorption–separation, nuclear waste immobilization, and applications including luminescence, magnetism, and microelectronics,[4,5,10,11] for example. The new material described here has been found by classical methods, but with the recent emergence and rapid development of artificial intelligence (AI) techniques and machine-learning (ML) models, the efficiency of materials discovery and property optimization may be improved.[12] The AI and ML methods can accelerate the screening of chemical compositions and analysis of the characterization data, and can be expected to further benefit sodalite-based materials' potential applications.[12–15] Sodalites therefore provide a promising route for the synthesis and modification of new zeolites and the exploration of their properties with different anion groups in the β-cage, and thus will be of future research interest.

In this report, we describe a previously unreported calcium aluminum rhenium sodalite (CARe sodalite) that we synthesized by a traditional high-temperature solid-state method. This solid-state synthesis method also works when preparing several different calcium aluminate sodalites (including chromium CACr, molybdenum CAMo, and tungsten CAW), but fails for sodium aluminosilicate sodalite with rhenium, as sodium rhenate ($NaReO_4$) forms first and then decomposes and evaporates before forming the sodalite structure. Finally, we also report that for the CARe sodalite, the rhenium in the sodalite β-cage is reducible under 5% H_2 forming gas, changing the material's color and yielding a stronger magnetic response.

Materials and methods

The polycrystalline CARe sodalite was prepared by a traditional high-temperature solid-state method in the air. Pre-dried calcium carbonate (Alfa Aesar Puratronic, 99.999%), aluminum oxide (Alfa Aesar. 99.98%), and rhenium metal powder (Alfa Aesar, -325 mesh, 99.99%) were mixed based on a stoichiometric ratio (with 5% excess Re due to its volatilization). The mixture was annealed at 1050°C for 3 days, and quench-cooled to room temperature in the furnace. Further grinding and annealing processes did not improve the material purity. The resulting

products were determined by powder X-ray diffraction (PXRD) to be a sodalite-type phase with a light yellow color, together with tiny amounts of calcium aluminate impurities. Different rhenium starting materials (i.e., ReO_3 and $Ca_5Re_2O_{12}$ precursors) were also employed and generated similar results. The reduced CARe sodalite was then obtained by annealing the as-made yellow sodalite powders under flowing forming gas (5% H2 + 95% Ar) at 700°C. The best reduction behavior was determined through use of the thermogravimetric analysis (TGA) technique on a TA Instruments TGA 5500 under 5% H2 in Ar.

Laboratory powder Xray diffraction (PXRD) patterns were collected using a Bruker D8 ADVANCE ECO with Cu Kα radiation ($\lambda = 1.5406$ Å). Rietveld refinements were conducted with GSAS II software on the collected PXRD patterns. For microstructure characterization by transmission electron microscopy (TEM), samples were prepared by dispersing dry CARe sodalite particles on TEM grids (Lacey carbon films with no formvar). Selected area electron diffraction (SAED), conventional TEM imaging, high-resolution scanning TEM (STEM) imaging, and energy-dispersive X-ray spectroscopy (EDS) mapping were performed on a double Cs-corrected FEI Titan Cubed Themis 300 scanning/transmission electron microscope, equipped with an X-FEG source and a Super-X energy-dispersive spectrometer.

UV–vis diffuse reflectance data were collected on an Agilent Cary 5000 spectrometer with Agilent Internal DRA-2500 diffuse reflectance accessory. The reflectance data were converted to absorption using the Kubelka–Munk function, and the band gap values are evaluated using Tauc plots. Magnetization and heat capacity measurements were carried out using a Quantum Design PPMS (DynaCool), equipped with a vibrating sample magnetometer (VSM) option.

Results and discussion

In spite of the complexity of the powder diffraction patterns of many zeolites,[1,3] that of the sodalite phase is relatively simple. The light yellow colored product powder obtained in the above reaction presents a sodalite-type structure with a powder diffraction pattern that fits the *I*-43 *m* cubic structure, which has been previously reported for many calcium aluminate sodalites.[8,16–18] Tiny amounts of impurities were also detected, while the main phase is estimated to be more than 90 wt% of the materials, as labeled in Fig. 1(a). To determine the stoichiometry of the sodalite, multiple batches with changing element ratios were prepared using the same synthesis conditions, and their products are compared by PXRD [Fig. 1(b)]. We found that a Ca-rich impurity ($Ca_{12}Al_{14}O_{33}$ = C12A7) increases when Al is deficient, while an Al-rich impurity ($CaAl_2O_4$) will be more prominent when there is not enough Ca in the system. Similarly, $Ca_5Re_2O_{12}$ is observed when too much Re is added in the starting material, in spite of some Re loss. The purest material is obtained with the metal ratio of Ca:Al:Re = 8:12:2. This ratio is consistent with the common sodalite formula, with fully filled β-cages, and is similar to the EDS results obtained from the STEM characterization (Figure S1). The elemental mapping also shows that the Re distribution in the particles is uniform. We found it to be very hard to make the product more pure than is shown in the figures. One possible explanation for this phenomenon is that due to the texture of the CARe sodalite powders, some small agglomerations of starting materials wrap the surfaces and thus hinder the complete reaction. This is further discussed in a later section of this report.

A Rietveld refinement carried out on the PXRD pattern [Fig. 1(a)] results in a unit cell of cubic *I*-43 *m* (#217) symmetry, $a = 9.28042(17)$ Å, $Z = 1$ (for $Ca_8Al_{12}O_{24}Re_2O_8$), and the refined results are presented in Table S1. TEM diffraction analysis confirmed the *I*-43 *m* symmetry and the lattice parameter of the cubic unit cell of the CARe sodalite [Fig. 1(c)]. Compared to other reported calcium aluminate sodalites (for $Ca_8Al_{12}X_2O_{32}$, $a = 9.22$ Å when $\boldsymbol{X}$ = Cr,[17] $a = 9.29$ Å for Mo,[8] and $a = 9.30$ Å for W[9]), the lattice parameter a of the CARe unit cell is not much different, consistent with the expectation that the size of the sodalite unit cell depends primarily on the size of the β-cage framework. It therefore also conversely confirms that when fabricating the CARe sodalite, the ionic group in the β-cage is different, while the cage framework is not changed much. Based on the refinement, the most optimized result is obtained with a ReO_4 tetrahedron in the sodalite cage with a small degree of disordering of its orientation, leading to a formula of $Ca_8Al_{12}Re_2O_{32}$ with Re(VI), consistent with many previously reported calcium aluminate sodalites. Compared to Re(VII), it is relatively rare to have Re(VI) in tetrahedral coordination with oxygen, so it may be that the unique sodalite framework restrains the coordination and forces the formation of $Re(VI)O_4$ in the cage. Alternatively, it may be actually Re(VII) in the ReO_4 tetrahedra, which would be more consistent with the magnetic susceptibility (will be further discussed later) which is more like what is expected for Re(VII) with no unpaired electrons. But that would require 0.5 extra O^{2-} in the cage per Re for charge neutrality, generating a more complicated coordination in place of a regular tetrahedron, which however is not possible to detect by X-ray diffraction due to the dominance of the X-ray scattering by the heavier elements present, and the Re–O polyhedron disorder. The calculated bond valence sum (BVS) for Re in the tetrahedron seen is 5.82, close to the suggested + 6 chemical valence. Therefore, a Re(VI) formula is demonstrated to be the formula for the as-made CARe sodalite, namely the material is $Ca_8Al_{12}Re_2O_{32} = Ca_8Al_{12}O_{24}(ReO_4)_2$. Further characterization has been carried out to study the rhenium chemical valence and behavior in the system, which will be discussed later. However, in order to more accurately locate the positions of oxygen atoms and confirm the chemical valence of rhenium, further structural characterization, such as neutron diffraction, which is more sensitive to oxygen, may be of future interest.

The as-made CARe sample was then reduced as described, resulting in a powder with a similar PXRD pattern but a dramatic color change, from light yellow to reddish brown, as shown in Fig. 2(a). A TGA experiment was then conducted

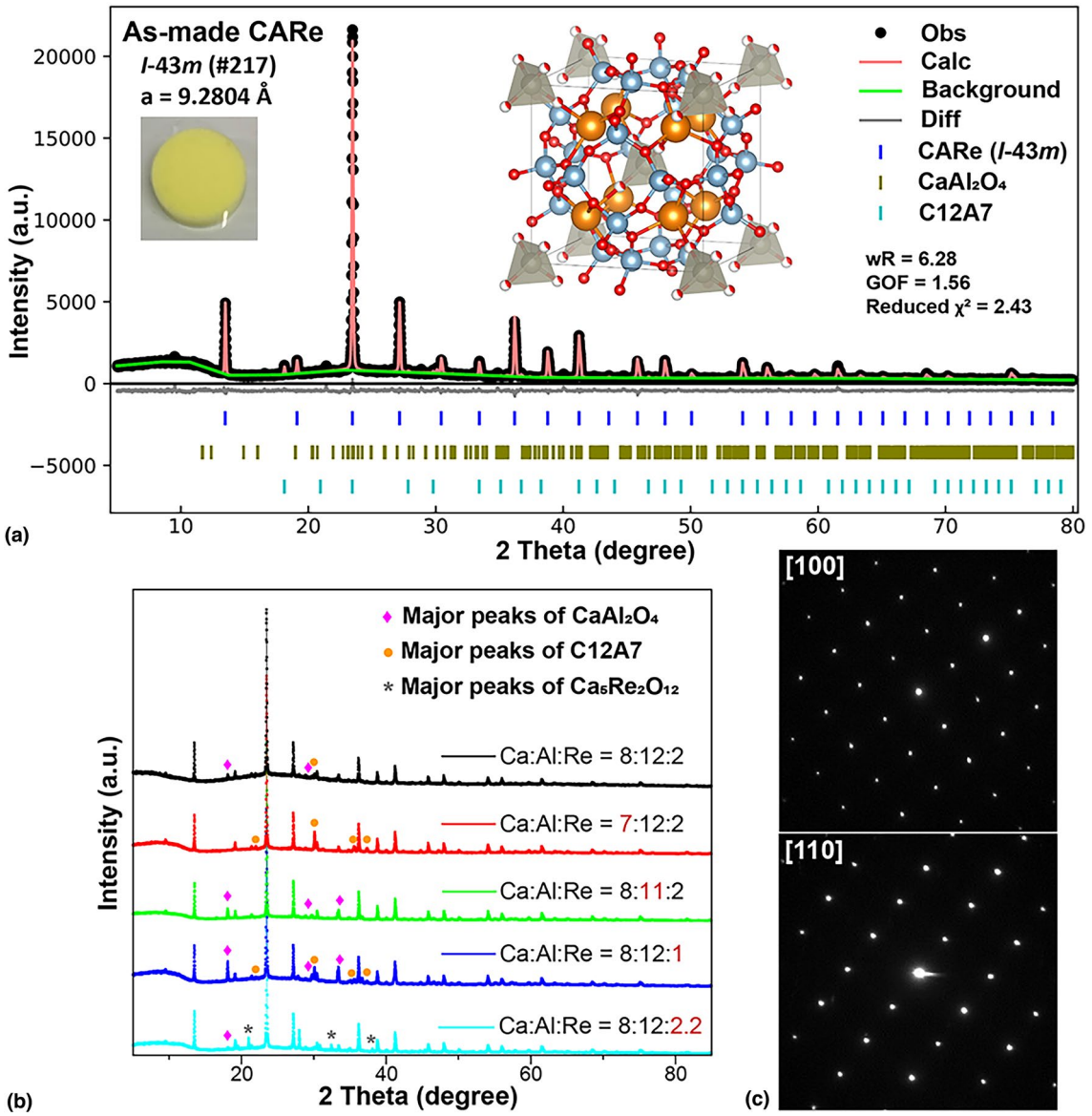

Figure 1. (a) Rietveld refinement of the laboratory PXRD pattern of the as-made CARe sodalite sample, with the image in the insets showing the sample color. The refined *I*-43 *m* unit cell is also presented, with Ca as orange spheres, Al as light-blue spheres, oxygen in red, and rhenium in gray (in the tetrahedra); The main CARe phase is refined to be more than 90.2 wt%; of the sample (b) The comparison of PXRD patterns of samples with different stoichiometries; (c) Electron diffraction patterns of the as-made CARe samples along the [100] and [110] directions, respectively. *I*-43 *m* symmetry was confirmed and the lattice parameter a was measured as 9.24 Å.

to determine how much oxygen was subtracted during the reduction. The TGA data show that the as-made CARe has some surface absorbed moisture present that can lead to a weight loss of 0.2%–0.3% at around 200°C regardless of the flowing gas. This is relatively common for some microporous structures and for Re-containing compounds,[19] and after getting rid of the surface moisture, the sample powder shows no difference in its color or its PXRD pattern. Thus, a reduction TGA test was carried out on the pre-dried as-made CARe powder under flowing 5% H_2/95% Ar gas, which was heated up to 700°C at 10°C/min and held isothermally for 10 h before fast cooling down. As shown in Fig. 2(b) and Figure S2, the weight of the CARe sample started to drop due to deoxygenation at around 500°C. Post-reduction PXRD confirmed that the sodalite cage structure has been maintained and thus that the Re in CARe is capable of intra-cage reduction (as is the case for CACr[16]). A TGA comparison was also conducted with other calcium aluminate sodalites (CAMo and CAW), data shown in Figure S2, suggesting that different from the case of CARe, CAMo and CAW show no obvious weight loss and thus show no sign of reduction under H_2/Ar up to a temperature of 700°C. CARe finally reached

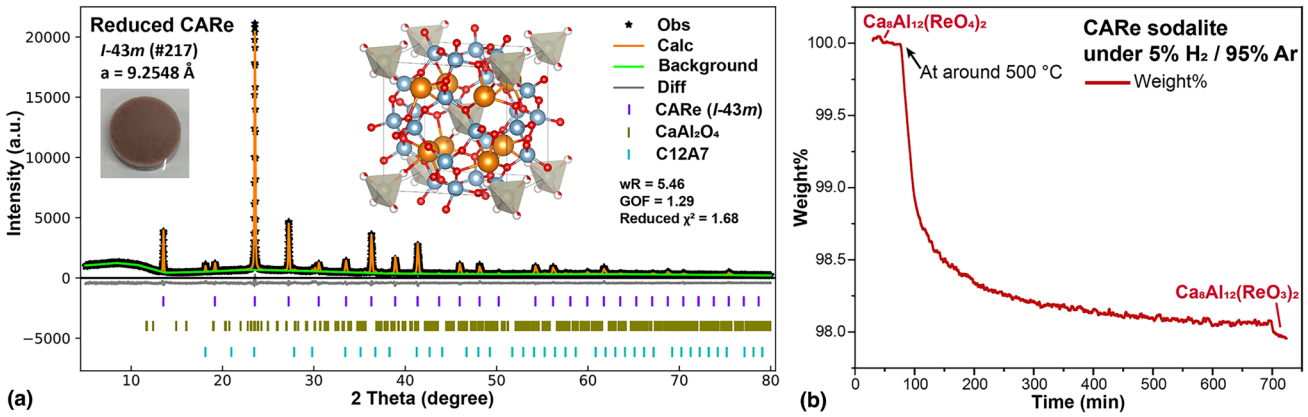

Figure 2. (a) Rietveld refinement of laboratory PXRD pattern of the reduced CARe sodalite sample, with the image in the insets showing the color change. The refined *I*-43 *m* unit cell is also presented, with Ca in orange, Al in light-blue, oxygen in red, and rhenium in gray (in the tetrahedra); The main CARe phase is refined to be more than 90.1 wt%; (b) The weight% vs time curve of TGA conducted on CARe sodalite sample under flowing 5% H_2/95% Ar forming gas.

a plateau at 97.97%. This is equal to 1.94 oxygen atoms per formula unit when we consider $Ca_8Al_{12}Re_2O_{32}$ as the formula of the as-made CARe. This makes the reduced CARe sodalite close to $Ca_8Al_{12}Re_2O_{30}$, with an oxygen-disordered Re(IV)O_3 tetrahedron in the β-cage. Noting that the measured weight percent drop is slightly smaller than the expected value of two oxygen losses per formula unit for Re(IV), it is possible that the reduction reaction is also not thoroughly completed in this process, leaving a small part of the sample not or not fully reduced. With the Re(IV) formula then fixed for the reduced material, a Rietveld refinement was done based on the PXRD of the reduced CARe sample [Fig. 2(a) and Table S1] giving an isostructural unit cell (#217 *I*-43 *m*) with a slightly smaller parameter $a = 9.25482(16)$ Å, consistent with the expectation of intra-cage reduction without breaking the sodalite framework. The Re–O bond length in the reduced sample is refined to be 1.94 Å, longer than the 1.83 Å of the as-made CARe. Further, the BVS is thus estimated to be 4.33, which is close to the +4 valence that is suggested for the Re in the reduced sodalite.

Although the *I*-43 *m* structural model yields a good Rietveld refinement for the as-made CARe sodalite, some very weak extra peaks are unmatched in the PXRD pattern, which may suggest that a sublattice or superstructure with lower symmetry compared to the *I*-43 *m* unit cell [Fig. 3(a)] is formed. The weakness of the extra diffraction peaks suggests that they may be due to oxygen ordering within the β-cages. For example, if the oxygen positions are correlated and the symmetry becomes *P*-43 m, then the body-centered symmetry is broken, and these reflections are matched [Fig. 3(a)]. It was confirmed by TEM diffraction analysis in Fig. 3(b) that some of the sodalite particles exhibit extra reflections which are forbidden in *I*-43 *m*. Therefore, the lower-symmetry particles, although in the minority, differ from the *I*-43 *m* ones in

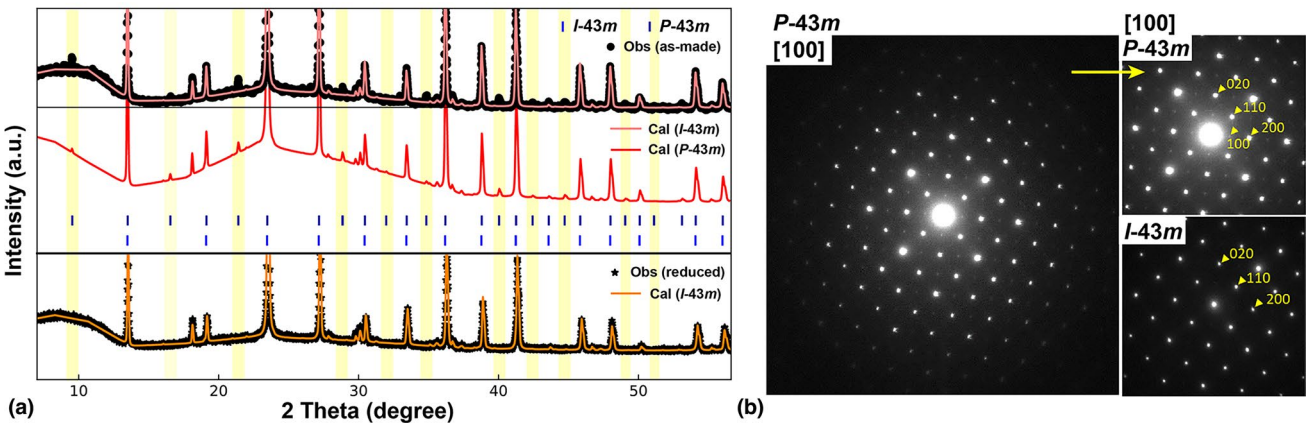

Figure 3. (a) PXRD of the as-made CARe sodalite, with calculated pattern in the space groups *I*-43 *m* and *P*-43 *m,* respectively. A comparison of reduced CARe PXRD pattern, together with its *I*-43 *m* calculated pattern, is also attached at the bottom. (b) Electron diffraction patterns of one particle in the as-made CARe sample show extra weak diffraction spots which correspond to a symmetry of *P*-43 *m*, as compared to the others with a symmetry of *I*-43 *m* in the same sample batch.

the as-made sample. We suppose that the reason for the symmetry breaking of some sodalite particles is possibly due to the off-centering or an orientational order/disorder transition of the ReO_4 polyhedra in the cage. This phenomenon is also observed in other calcium aluminate sodalites, as with decreasing temperatures, the XO_4 tetrahedron can undergo a transition from disordered to ordered, accompanied in some cases by a degradation from cubic, to tetragonal, and finally orthorhombic symmetry.[17,20–22] These tiny extra peaks are absent in the reduced CARe pattern, which further supports the suggestion that it is the position-off or orientational ordering of the in-cage ReO_4 tetrahedra that lower the symmetry from body-centered cubic. As the reduction subtracts some oxygen from ReO_4 and increases the degree of disorder, these sublattice peaks disappear and the system displays an *I*-43 *m* cubic structure.

Diffuse reflectance measurements were carried out on both the as-made and reduced CARe sodalites. In Fig. 4(a) a single transition is detected for the as-made sample, while two transitions can be observed in the reduced CARe sample. The band gaps are estimated using Tauc plots [Fig. 4(a) inset] with the equation[23,24]:

$$(\alpha h\nu)^n = A(h\nu - E_g), \quad (1)$$

where A is a constant, α is the absorption coefficient (cm^{-1}), and $n=2$ for direct transitions, 0.5 for indirect transitions. Correlating with their sample colors, the absorption between 600 and 900 nm is attributed to the reduced phase, and their transitions are suggested to be indirect (also consistent with the light-colored powder the as-made sample). Therefore, the values of the band gaps are estimated to be 2.59 eV for the as-made CARe with its light yellow color, and 1.50 eV for reduced CARe with its reddish brown color.

Finally, the temperature-dependent magnetic susceptibilities (χ=M/H) were measured from 1.8 to 300 K under 1000 Oe applied fields for both the as-made and reduced CARe. The data are presented in Fig. 4(b), with an enlarged view in the inset. Both samples show paramagnetic behavior at lower temperature (although the magnetic susceptibility is much weaker for the as-made sample) with an upturn in magnetic susceptibility, and a much smaller signal (very close to zero) in the high-temperature range. The reduced sample shows dramatically higher magnetic response compared to the as-made one at lower temperature, which, when considering the tetrahedral coordination model adopted in this report, suggests a high-spin electron configuration of Re(+4) after reduction. The behavior of both CARe sodalites, especially in the high-temperature range, is weaker than expected for the Curie–Weiss Law. This may suggest that an interesting spin/orbit interaction is present. We note that the shortest distance between two magnetic centers (i.e., the Re) is around 8 Å in the CARe unit cell, and one potential possibility, although not expected, is that magnetic centers with one unpaired electron (i.e., Re(VI)) are paired with each other above 300 K,

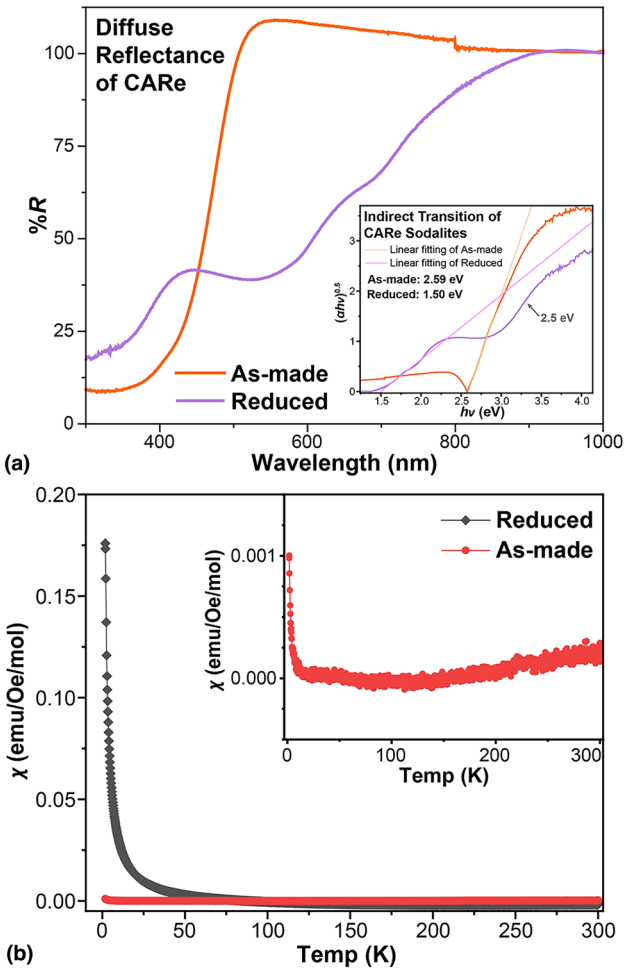

Figure 4. (a) Diffuse reflectance spectra of the as-made and reduced CARe sodalite samples, with a Tauc plot of indirect transitions in the inset. (b) Magnetic susceptibility characterization of the as-made and reduced CARe sodalites, measured under an applied field of 1000 Oe. A zoomed-in view for the as-made sample is shown in the inset.

thus leaving behind a low magnetic susceptibility. Whatever is the case at the magnetic level, the newly discovered calcium aluminum rhenium sodalite can be reduced while maintaining the cage framework, further extending the versatility of the sodalite compositions, and shows that the sodalite β-cage structure is able to host atypical behavior that may be of interest for future study and inspire the fabrication of new functional materials.

Conclusions

A newly reported calcium aluminum sodalite, with rhenate polyhedra in the β-cage (CARe sodalite), has been synthesized by a traditional high-temperature solid-state method. The rhenium in the sodalite cage can be reduced to a lower

chemical valence under 5% H_2 forming gas without breaking the sodalite framework, leading to variations in the optical and magnetic properties of the compound. Preliminary characterization is conducted. The CARe system described here is an indication of the diversity of the sodalite structure. The variation of the ionic group in the sodalite β-cage with the addition of the distinctive caged framework can result in interesting and varying properties, and provide more insight into new material design and fabrication. Future work is suggested, in particular to determine the oxygen content and distribution in this material by neutron diffraction.

Acknowledgments

This work was supported by the Gordon and betty Moore Foundation grant number GBMF-9066. The authors acknowledge the use of Princeton's Imaging and Analysis Center, which is partially supported by the Princeton Center for Complex Materials, a National Science Foundation (NSF)-MRSEC program (DMR-2011750).

Author contribution

Danrui Ni contributed toward conceptualization, methodology, investigation, formal analysis, visualization, and writing—original draft; Guangming Cheng contributed toward validation, investigation, formal analysis, visualization, and writing—reviewing and editing; Lun Jin contributed toward validation, investigation, and formal analysis; Chen Yang contributed toward validation and investigation; Nan Yao contributed toward resource, supervision, and project funding acquisition; Robert J. Cava* contributed toward conceptualization, resource, supervision, project funding acquisition, administration, and writing- reviewing and editing.

Funding

This study was funded by Gordon and betty Moore Foundation Grant Number GBMF-9066 and National Science Foundation (NSF)-MRSEC program (DMR-2011750).

Data availability

Data will be available on request from the authors.

Declarations

Competing interest

The authors declare that they have no known competing financial interests or personal relationships that could have appeared to influence the work reported in this paper.

Supplementary Information

The online version contains supplementary material available at https://doi.org/10.1557/s43579-024-00550-7.

References

1. D.W. Breck, *Zeolite Molecular Sieves: Structure, Chemistry, and Use* (Wiley, New York, 1973)
2. A.R. West, *Solid State Chemistry and Its Applications*, 2nd edn. (Wiley, New York, 2022)
3. T. Weller M, Where zeolites and oxides merge: semi-condensed tetrahedral frameworks. J. Chem. Soc. Dalton Trans. **5**, 4227–4240 (2000). https://doi.org/10.1039/B003800H
4. J. Li, A. Corma, J. Yu, Synthesis of new zeolite structures. Chem. Soc. Rev. **44**, 7112–7127 (2015). https://doi.org/10.1039/C5CS00023H
5. W. Depmeier, The sodalite family: a simple but versatile framework structure. Rev. Mineral. Geochem. **57**, 203–240 (2005). https://doi.org/10.2138/rmg.2005.57.7
6. M.E. Brenchley, M.T. Weller, Synthesis and structure of sulfide aluminate sodalites. J. Mater. Chem. **2**, 1003–1005 (1992). https://doi.org/10.1039/JM9920201003
7. M.E. Brenchley, M.T. Weller, Structures of strontium selenite and strontium selenide aluminate sodalites and the relationship of framework structure to vibrational spectra in aluminate sodalites. Chem. Mater. **5**, 970–973 (1993). https://doi.org/10.1021/cm00031a015
8. S. van Smaalen, R. Dinnebier, H. Katzke, W. Depmeier, Structural characterization of the high-temperature phase transitions in $Ca_8[Al_{12}O_{24}](MoO_4)_2$ aluminate sodalite using x-ray powder diffraction. J. Solid State Chem. **129**, 130–143 (1997). https://doi.org/10.1006/jssc.1996.7251
9. W. Depmeier, Structure of cubic aluminate sodalite $Ca_8[Al_{12}O_{24}](WO_4)_2$ in comparison with its orthorhombic phase and with cubic $Sr_8[Al_{12}O_{24}](CrO_4)_2$. Acta Cryst. B **44**, 201–207 (1988). https://doi.org/10.1107/S0108768187011959
10. S. Lee, H. Xu, H. Xu, R. Jacobs, D. Morgan, Valleyite: a new magnetic mineral with the sodalite-type structure. Am. Miner. **104**, 1238–1245 (2019). https://doi.org/10.2138/am-2019-6856
11. B.K. Singh, M.A. Hafeez, H. Kim, S. Hong, J. Kang, W. Um, Inorganic waste forms for efficient immobilization of radionuclides. ACS EST Eng. **1**, 1149–1170 (2021). https://doi.org/10.1021/acsestengg.1c00184
12. A. Merchant, S. Batzner, S.S. Schoenholz, M. Aykol, G. Cheon, E.D. Cubuk, Scaling deep learning for materials discovery. Nature **624**, 80–85 (2023). https://doi.org/10.1038/s41586-023-06735-9
13. L.T. Glasby, E.H. Whaites, P.Z. Moghadam, Machine learning and digital manufacturing approaches for solid-state materials development. In: AI-Guided Design and Property Prediction for Zeolites and Nanoporous Materials. Wiley, pp 377–409 (2023)
14. R.P. Xian, V. Stimper, M. Zacharias, M. Dendzik, S. Dong, S. Beaulieu, B. Schölkopf, M. Wolf, L. Rettig, C. Carbogno, S. Bauer, R. Ernstorfer, A machine learning route between band mapping and band structure. Nat. Comput. Sci. **3**, 101–114 (2023). https://doi.org/10.1038/s43588-022-00382-2
15. J.M. Gregoire, L. Zhou, J.A. Haber, Combinatorial synthesis for AI-driven materials discovery. Nat Synth **2**, 493–504 (2023). https://doi.org/10.1038/s44160-023-00251-4
16. D. Ni, Z. Hu, G. Cheng, X. Gui, W.-Z. Yu, C.-J. Jia, X. Wang, J. Herrero-Martín, N. Yao, L.-H. Tjeng, R.J. Cava, Magnetic frustration in a zeolite. Chem. Mater. **33**, 9725–9731 (2021). https://doi.org/10.1021/acs.chemmater.1c03500
17. S.M. Antao, I. Hassan, J.B. Parise, Chromate aluminate sodalite, $Ca_8[Al_{12}O_{24}](CrO_4)_2$: phase transitions and high-temperature structural evolution of the cubic phase. Can. Mineral. **42**, 1047–1056 (2004). https://doi.org/10.2113/gscanmin.42.4.1047

18. I. Hassan, Structural modulations in a pseudo-cubic aluminate sodalite, $Ca_8[Al_{12}O_{24}](CrO_4)_2$. Z. Kristallogr. **211**, 228–233 (1996). https://doi.org/10.1524/zkri.1996.211.4.228
19. M.T. Greiner, T.C.R. Rocha, B. Johnson, A. Klyushin, A. Knop-Gericke, R. Schlögl, The oxidation of rhenium and identification of rhenium oxides during catalytic partial oxidation of ethylene: an in-situ XPS study. Z. Phys. Chem. **228**, 521–541 (2014). https://doi.org/10.1515/zpch-2014-0002
20. I. Hassan, Direct observation of phase transitions in aluminate sodalite, $Ca_8[Al_{12}O_{24}](CrO_4)_2$. Am. Miner. **81**, 1375–1379 (1996). https://doi.org/10.2138/am-1996-11-1210
21. I. Hassan, Aluminate socialite, $Ca_8[Al_{12}O_{24}](CrO_4)_2$, with tetragonal and orthorhombic superstructures. Eur. J. Mineral. **8**, 477–486 (1996)
22. R. Melzer, W. Depmeier, A structural study of aluminate sodalite $Ca_8[Al_{12}O_{24}](CrO_4)_2$ (CACr). Cryst. Res. Technol. **31**, 459–467 (1996). https://doi.org/10.1002/crat.2170310409
23. J. Tauc, R. Grigorovici, A. Vancu, Optical properties and electronic structure of amorphous germanium. Phys. Status Solidi B **15**, 627–637 (1966). https://doi.org/10.1002/pssb.19660150224
24. J. Tauc, Optical properties and electronic structure of amorphous Ge and Si. Mater. Res. Bull. **3**, 37–46 (1968). https://doi.org/10.1016/0025-5408(68)90023-8